1106

LIQUEFACTION AND SETTLEMENT OF AN IMPROVED GRAVELLY FILL OF WEATHERED GRANITE DURING STRONG EARTHQUAKE

Y GOTO[1] And K ITO[2]

SUMMARY

During the 1995 Hyogoken-Nanbu Earthquake, there was a slight damage due to liquefaction in a weathered granite fill (called Masado) improved by rod compaction method and a severe damage in an unimproved fill. The liquefaction and settlement characteristics of the improved fill of weathered granite were estimated from the laboratory soil test with the undisturbed frozen sample and the earthquake response analysis based on the effective stress method considering the compressibility of soil during post-liquefaction. The liquefaction strength and compression index of the improved fill before and post-liquefaction were compared with the laboratory test results with the undisturbed frozen sample obtained from the unimproved fill. These mechanical properties were incorporated into the constitutive model of soil. The analytical results on the improved and the unimproved ground were compared with the liquefaction phenomena actually observed and the residual settlement obtained from leveling measurement conducted after the earthquake. On the laboratory test results, the liquefaction strength of the improved fill is one and a half time as large as that of the unimproved fill. The compression index during post-liquefaction shows almost the same value on the improved and the unimproved fill. On the analytical results, liquefaction was occurred at G.L-7 m or deeper of the Masado fill in the improved ground, while occurred at all depth (18 m) of it in the unimproved ground. Both of the analytical and the actually observed results imply that settlement of the improved ground is 7 to 8 cm and it is reduced against 32 cm actually observed on the unimproved ground. From these results, the soil improvement by rod compaction method resulting in higher liquefaction strength was effective to reduce the damages induced by liquefaction. The residual settlement induced by liquefaction was properly predicted under the effective stress method considering the effect of soil improvement and the characteristics of compressibility of soil during post-liquefaction.

INTRODUCTION

The unimproved gravelly fill of weathered granite (called Masado) in Port Island was experienced severe damage of liquefaction accompanying with large ground deformation and sand boils during the 1995 Hyogoken-nanbu earthquake. On the other hand, neither ground deformation such as large residual settlement nor sand boil was observed in the gravelly fill of weathered granite improved by rod compaction method. Based on the investigations after the 1995 Hyogoken-nanbu earthquake concerned with the some types of soil improvement, the effectiveness of soil improvement was confirmed [Yasuda et al., 1995]. Under these considerations, the liquefaction characteristics of sand with relatively large SPT-*N* value and the improved ground against soil liquefaction will be of great interest for engineers, because the soil had been believed not to liquefy under conventional design specification compiled before this earthquake.

In such a situation, firstly, the physical and mechanical properties of intact samples taken by in-situ freezing sampling at the improved ground by rod compaction method were compared with those taken at the unimproved site in order to clarify the effectiveness of soil improvement against liquefaction and residual settlement.

[1] *Technical Research Institute of Obayashi Corporation, Tokyo, Japan Email:KGE00351@nifty.ne.jp*
[2] *Technical Research Institute of Obayashi Corporation, Tokyo, Japan Email:itohj@o-net.obayashi.co.jp*

Secondly, two types of one-dimensional effective stress analysis were performed, one is for the improved ground and the another is for the unimproved ground where in-situ freezing samplings were conducted.
On these analyses, the physical and mechanical properties, model parameters utilized in constitutive model of soils were determined based on the in-situ test and detailed laboratory soil tests with intact samples and input ground motion at the bedrock in engineering sense were determined from the downhole strong motion actually observed. These analytical results were compared with the actually observed results on liquefaction and residual settlement at these improved and unimproved fills during the 1995 Hyogoken-nanbu earthquake.

LIQUEFACTION AND SETTLEMENT CHARACTERISTICS OF IMPROVED FILL

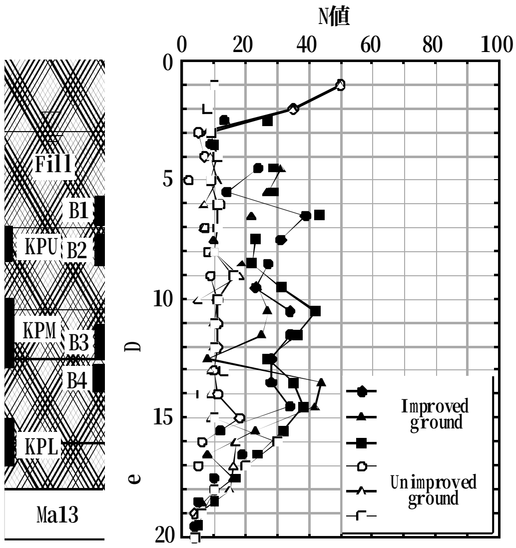

Figure 2: Distribution of SPT N-value

The location of the improved site and the unimproved site is shown in Figure 1. The former was investigated by the Japanese companies and universities organized cooperative research group named Geotechnical Research Collaboration Committee on the Hanshin-Awaji Earthquake [Geotechnical Research Collaboration Committee on the Hanshin-Awaji Earthquake, 1998]. The latter is located at a point approximately 200 m south of the investigated point of the former and was investigated by Hatanaka et al. [Hatanaka et al., 1997, Suzuki et al., 1997, Uchida et al., 1998]. The downhole strong motion observation station of Kobe City is located at an unimproved area approximately 130 m south of the investigated point of the improved site [Kobe City, 1995]. The SPT N-values on the improved ground and the unimproved ground, the sampling depth of intact samples taken by the in-situ freezing sampling are shown in Figure 2. The SPT N-values on the unimproved ground ranges from 5 through 20 and the SPT N-values on the improved ground are increased up to 20 through 35.

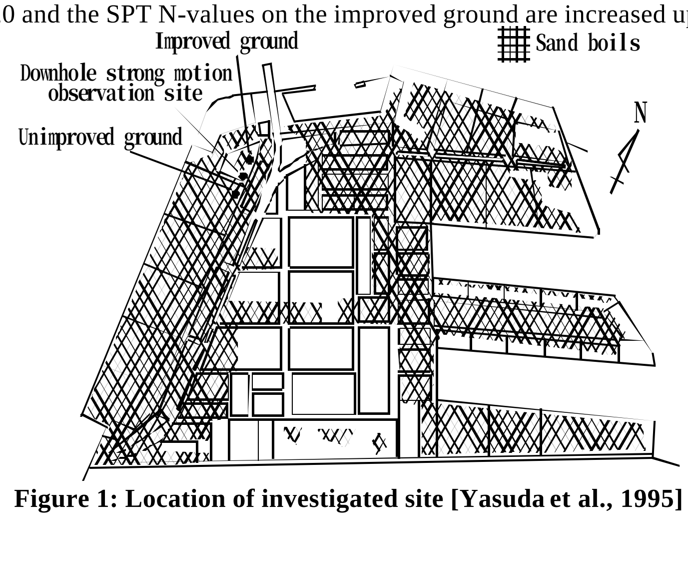

Figure 1: Location of investigated site [Yasuda et al., 1995]

The undrained cyclic triaxial tests are performed with intact samples B1 through B4 for the improved fill and with intact samples KPU through KPL for the unimproved fill. The comparison in the relationship between liquefaction strength at DA = 5 % and the number of cycles is shown in Figure 3 for the improved and the unimproved fill. The liquefaction strength for the improved fill is almost one and a half time as large as that for the unimproved fill. The liquefaction strengths R5 and R20 at DA = 5 % obtained from Figure 3 are compared with design curve in Design Specifications of Highway Brides compiled by the Ministry of Construction [Japan Road Association, 1996] in Figure 4. The liquefaction strength vs. Corrected N-value relationships by design specification and test results shows similar tendency, but absolute value is a little smaller in the test than in the design specification. With sample B4 for the improved fill and sample KPL for the unimproved fill, the relationships between volumetric strain and confining stress under initial consolidation process on the triaxial tests are shown in Figure 5. The relationships between volumetric strain and effective mean stress under drainage process on the undrained cyclic triaxial tests for mv are shown in Figure 6. The compression index Cc/1+e0 represented in Figures 5 and 6 is determined from the initial gradient on the relationship between volumetric strain and confining stress, effective mean stress with exponent of power function 0.5. The averaged Cc/1+e0 with samples B1 through B4 for the improved fill and with samples KPU through KPL for the unimproved fill are 0.009 and 0.014 under consolidation process and 0.021 and 0.018 under drainage process. The difference in compression index is large under consolidation process between the improved and the unimproved ground, while the compression index is almost same under drainage process. This characteristic of the compressibility during post-liquefaction to be mentioned above is incorporated into the constitutive model of soil, which is in the form of depending on the change of effective mean stress.

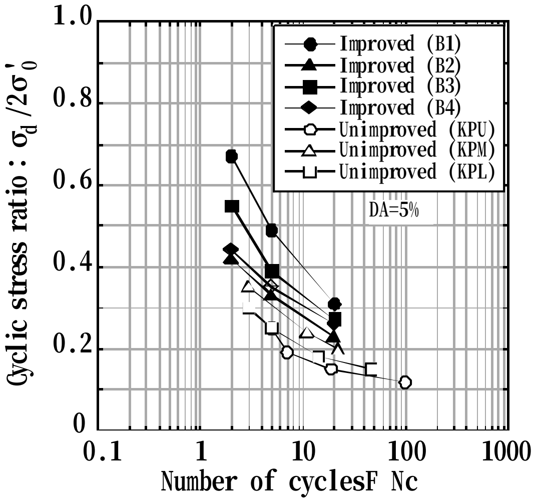

Figure 3: Comparison of liquefaction strength

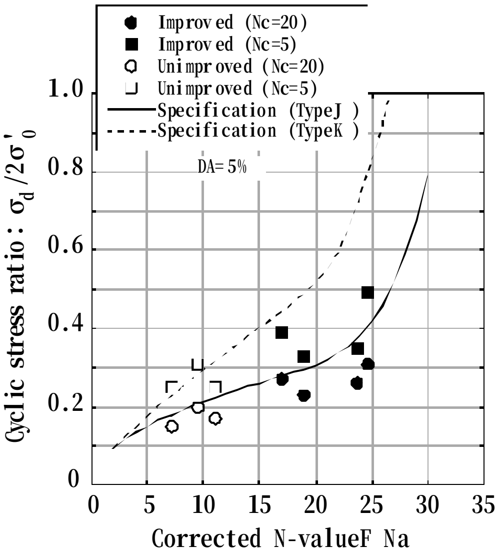

Figure 4: Comparison of liquefaction strength

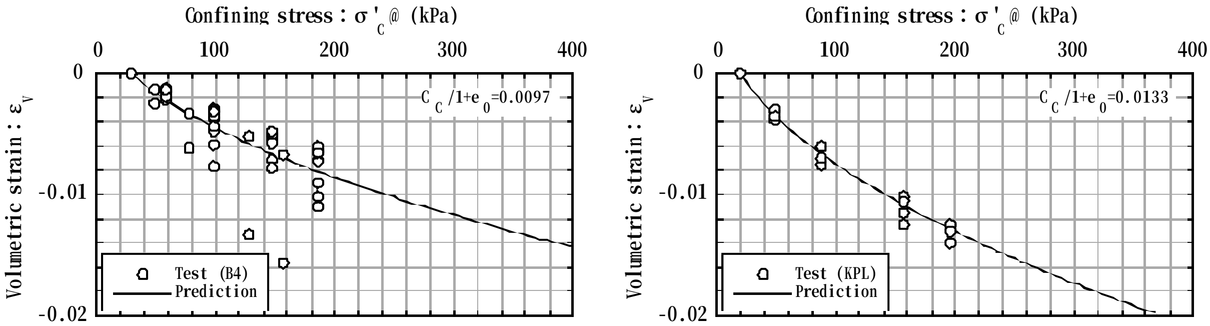

Figure 5: Volumetric strain under consolidation process for improved and unimproved fill

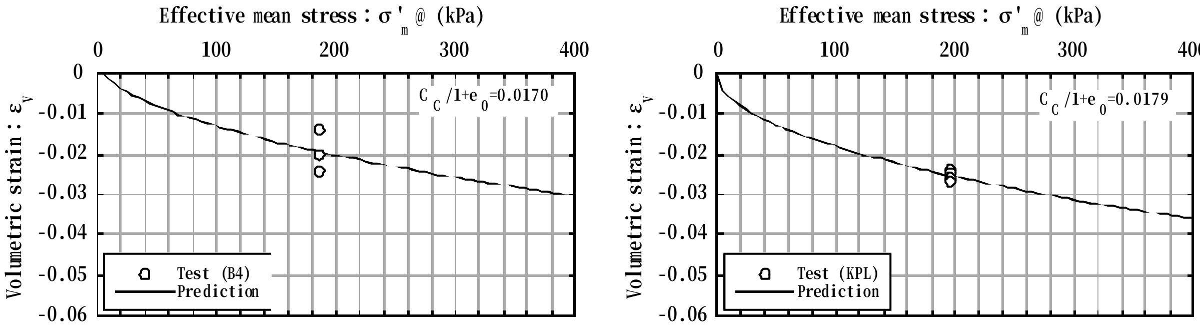

Figure 6: Volumetric strain under drainage process for improved and unimproved fill

ONE DIMENSIONAL EFFECTIVE STRESS ANALYSIS

Analytical Model

The analytical models for the improved and the unimproved ground are shown in Figure 7. In the improved ground, the fill is divided into the improved layers B1 through B4 and the unimproved layer B5 rested at G.L.-16 m through G.L.-18 m based on the depth of freezing sampling and the distribution of the SPT N-value as shown in Figure 2. In the unimproved ground, the fill is divided into layers B1 through B3 based on the depth of freezing sampling. The coefficient of earth pressure at rest K0 is set to 0.5 for the unimproved fill and 0.8 for the improved fill [Geotechnical Research Collaboration Committee on the Hanshin-Awaji Earthquake, 1998].
3.2 Physical and Mechanical Soil Properties

The representative physical and mechanical soil properties are shown in Tables 1 and 2. The soil properties for the improved layer B1 through B4 are determined from P-S logging, test results obtained from laboratory soil tests with intact samples [Geotechnical Research Collaboration Committee on the Hanshin-Awaji Earthquake, 1998]. The soil properties for the unimproved layer B1 through B3 and B5 are determined from test results investigated by Hatanaka et al. [Hatanaka et al., 1997, Suzuki et al., 1997, Uchida et al., 1998].

Table 1: Soil properties for improved ground

Soil type	Depth m	ρ_t t/m³	V_s m/s	ρ_s t/m³	e	k cm/s	R_{20}	ϕ_p °	ϕ_f °	$(C_c/1+e_0)_i$	$(C_c/1+e_0)_l$
B1	-3	1.98	140	2.60	0.31	1.5×10^{-3}	0.31	33.5	42.3	0.0081	0.0184
	-7	2.22	190								
B2	-10	2.20	210	2.62	0.35	1.2×10^{-3}	0.23	32.1	42.4	0.0077	0.0274
B3	-13	2.23	220	2.61	0.31	2.2×10^{-3}	0.27	32.6	43.3	0.0099	0.0209
B4	-16	2.18	250	2.62	0.37	1.8×10^{-3}	0.26	33.1	42.0	0.0097	0.0170
B5	-18	2.20	220	2.63	0.355	1.1×10^{-2}	0.17	33.1	39.8	0.0133	0.0179
A_c	-28	1.6	180	2.60	1.65	1.0×10^{-6}	—	—	35.0	—	—
A_g	-32	1.8	245	2.60	1.0	1.0×10^{-6}	—	—	38.0	—	—

Table 2: Soil properties for unimproved ground

Soil type	Depth m	ρ_t t/m³	V_s m/s	ρ_s t/m³	e	k cm/s	R_{20}	ϕ_p °	ϕ_f °	$(C_c/1+e_0)_i$	$(C_c/1+e_0)_l$
B1	-3	1.89	140	2.62	0.385	2.0×10^{-3}	0.15	33.5	41.8	0.0152	0.0191
	-7.5	2.17	170								
B2	-15	2.16	200	2.63	0.40	1.1×10^{-2}	0.20	32.4	39.5	0.0125	0.0173
B3	-18	2.20	220	2.63	0.355	1.1×10^{-2}	0.17	33.1	39.8	0.0133	0.0179
A_c	-28	1.6	180	2.60	1.65	1.0×10^{-6}	—	—	35.0	—	—
A_g	-32	1.8	245	2.60	1.0	1.0×10^{-6}	—	—	38.0	—	—

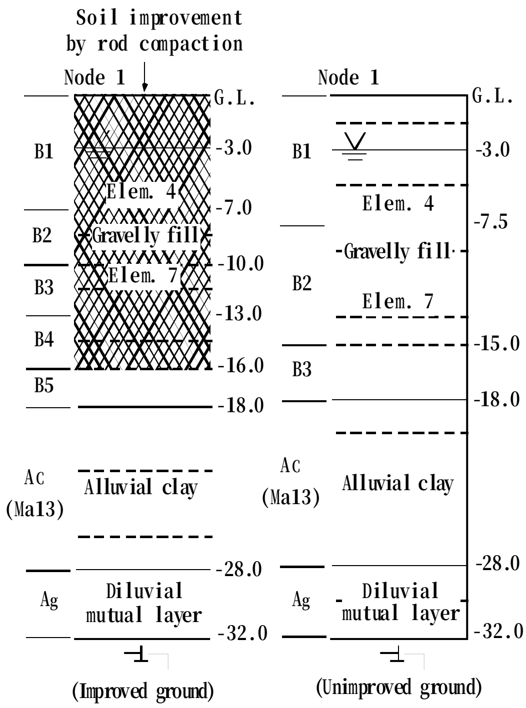

Figure 7: Analytical model

PARAMETERS FOR CONSTITUTIVE MODEL OF SOIL

The constitutive model of soil proposed by Prof. Matuoka is adopted in the analyses [Ito, 1995]. The parameters for constitutive model is determined from drained triaxial compression test (CD). The CD test results obtained from the improved layer B1 is shown in Figure 8. After subtracting plastic volumetric strain caused by isotropic consolidation and elastic strain from total strain, the relationship between deviator stress and plastic strain caused by only shear is shown in Figure 9. The relationship between shear to normal stress ratio and plastic shear strain increment ratio on mobilized plane corresponding to the stress-dilatancy relationship is shown in Figure 10. The two of dilatancy parameters are determined from the gradient and the intercept and these values are related to the phase transformation angle in Equation (1).

$$\tan \phi_p = \frac{2m}{2-l} \tag{1}$$

$$k_S = k_{S,ref} \times \sqrt{\frac{\sigma'_{mi}}{\sigma'_{mi,ref}}} \tag{2}$$

The relationship between shear to normal stress ratio and maximum plastic shear strain on mobilized plane is shown in Figure 11. The hardening parameter is determined from the reciprocal of initial gradient. As shown in Figure 11, the hardening parameter is set to be in proportion to the initial effective mean stress in the form of Equation (2) with exponent of power function 0.5 in the analyses.

The comparisons between the undrained cyclic triaxial test results at the improved layer B2 and the analytical results under undrained simple shear condition concerned with model parameters to be determined above are shown in Figures 12 and 13.

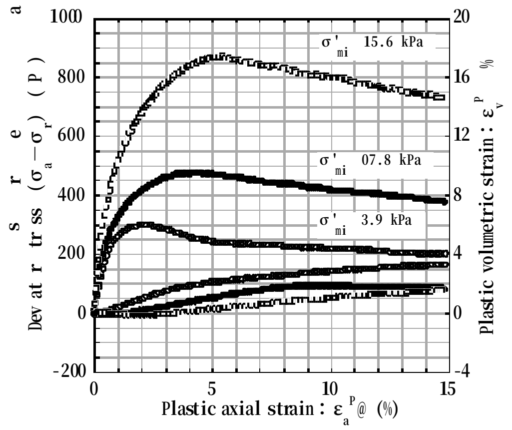

Figure 9: Deviator stress, plastic volumetric strain vs. plastic axial strain (B1)

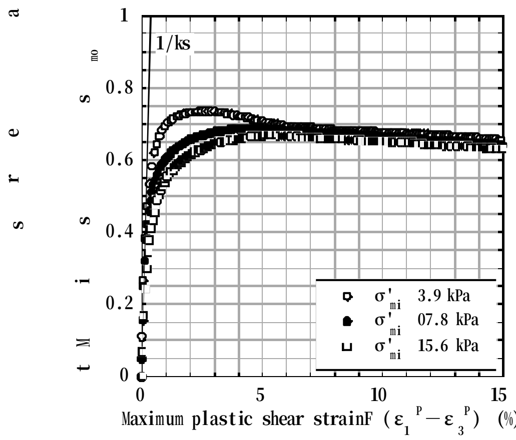

Figure 11: Shear to normal stress ratio vs. maximum plastic shear strain (B1)

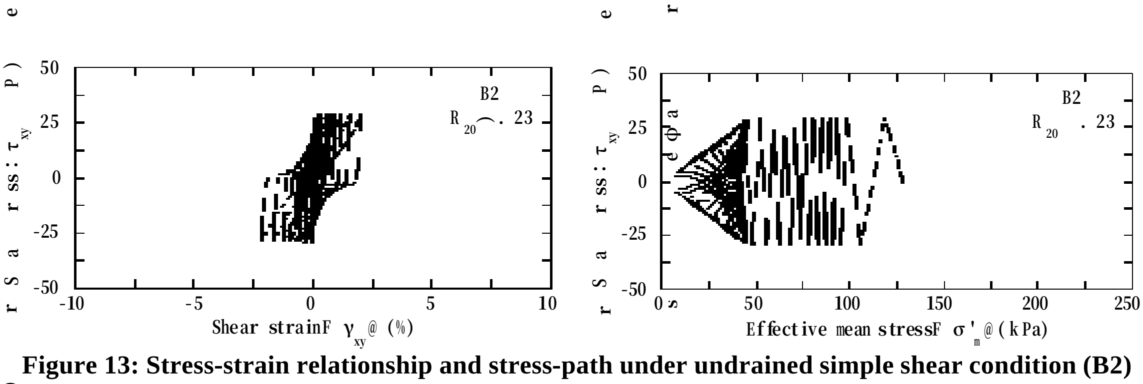

Figure 13: Stress-strain relationship and stress-path under undrained simple shear condition (B2)

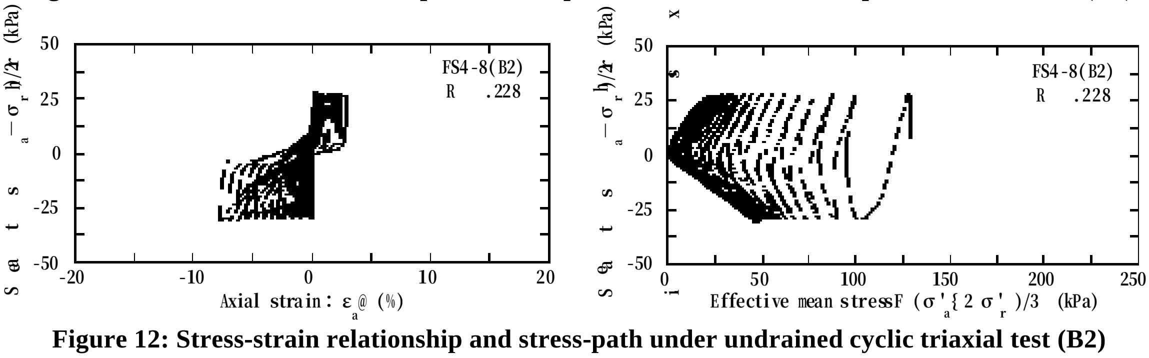

Figure 12: Stress-strain relationship and stress-path under undrained cyclic triaxial test (B2)

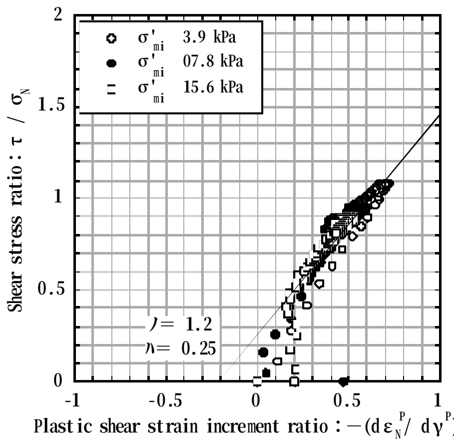

Figure 10: Shear to normal stress ratio vs. normal to plastic shear strain increment (B1)

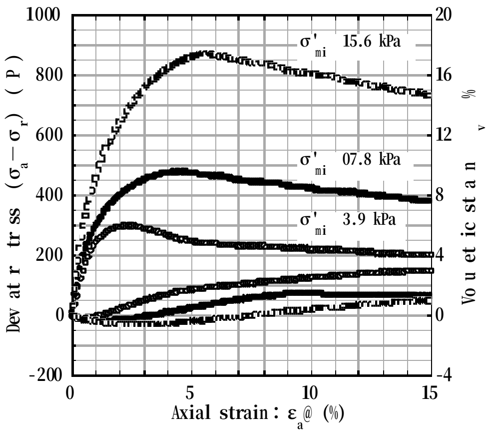

Figure 8: Deviator stress, total volumetric strain vs. axial strain (B1

INPUT GROUND MOTION

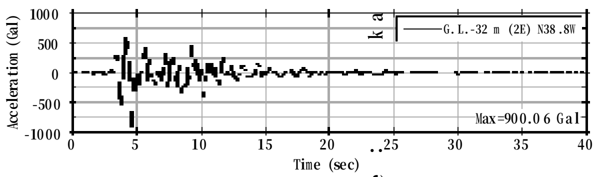

Figure 15: Time histories of acceleration (G.L.-32 m (2E))

The bedrock in the engineering sense is set to be at the depth of G.L.-32 m where ground motion records were obtained by the strong motion observation station of Kobe City just neighboring the investigated site during the 1995 Hyogoken-nanbu earthquake [Kobe City, 1995]. The incident wave (2E) at the depth of G.L.-32 m during the earthquake is computed by means of equivalent linear method using the ground motion records at the depth of G.L.-32 m and G.L.-83 m actually observed. The time histories of ground motion at G.L.-32 m and G.L.-83 m synthesized to N38.8W are shown in Figure 14 and the time history of the incident wave (2E) at the depth of G.L.-32 m to be derived is shown in Figure 15.

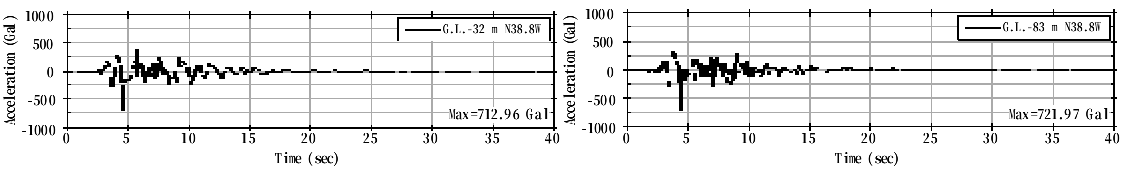

Figure 14: Time histories of acceleration (G.L.-32 m and G.L.-83 m)

ANALYTICAL RESULTS

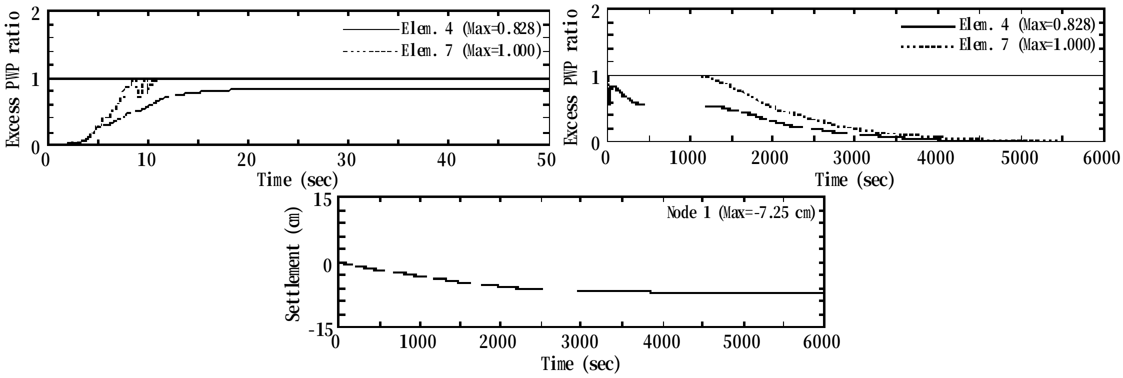

Figure 16: Time histories of excess pore-water pressure ratio and residual settlement (improved)

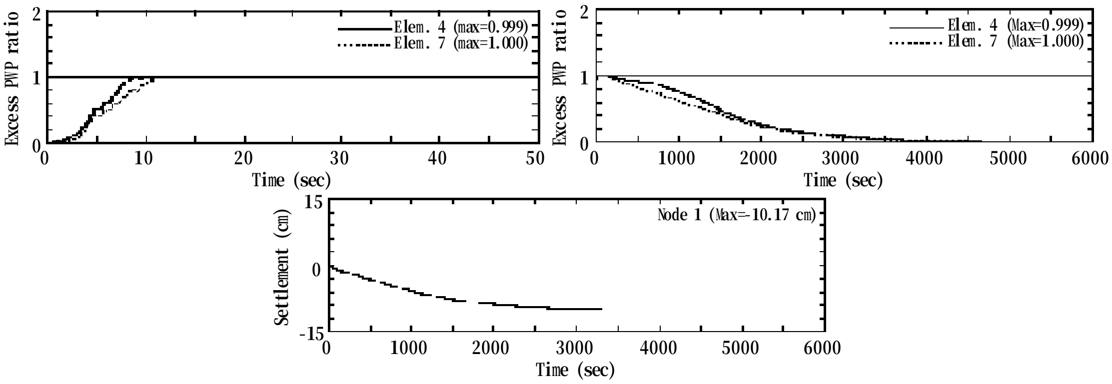

Figure 17: Time histories of excess pore-water pressure ratio and residual settlement (unimproved)

The time histories of excess pore-water pressure ratio in layers B1 (Element 4) and B3 (Element 7) at the improved ground and in layers B1 (Element 4) and B2 (Element 7) at the unimproved ground are shown in Figures 16 and 17 during 50 sec and 6000 sec. The liquefaction is occurred in all layers B1 through B5 at the unimproved ground. On the other hand, the liquefaction is occurred in layers B2 through B5 but is not occurred in layer B1 of G.L.-7 m or shallower at the improved ground. This agrees well with the actual liquefaction phenomenon judged from observation of sand boils on the ground surface. The time histories of ground settlement at the improved and the unimproved ground are shown in Figures 16 and 17 during 6000 sec. It takes about 1 through 1.5 hours for excess pore-water pressure to be dissipated completely, resulting in the residual settlement of 7 cm on the ground surface at the improved ground and 10 cm at the unimproved ground. The compression index during post-liquefaction at the improved fill and the unimproved fill is almost same as shown in Tables 1 and 2. The reason why the ground settlement at the improved ground is smaller is that the liquefaction is not occurred in all the depth of the fill.

RESIDUAL SETTLEMENT OF IMPROVED GROUND

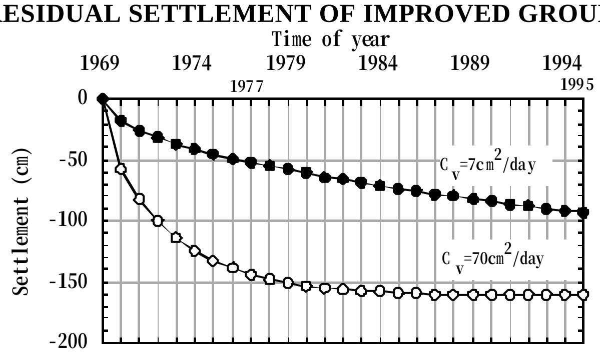

Figure 19: Time history of settlement for Ma13

The results of relative settlement of the buildings by leveling measurement after the 1995 Hyogoken-nanbu earthquake is shown in Figure 18, which management office building supported by tip-support piles is regarded as a reference level. The values of Figure 18 include the consolidation settlement for alluvial clay (Ma13) from the time of construction of structure (1977) to the earthquake (1995). On the condition that the coefficient of volume compressibility mv is 0.07 cm2/kgf, the coefficient of consolidation Cv is 70 cm2/day and 7 cm2/day, the consolidation curve is represented in Figure 19 from the time of reclamation (1969) to the earthquake [Kobe City, 1995]. The averaged consolidation settlement for Ma13 is roughly estimated to be 29 cm as shown in Figure 19, which may have occurred during its corresponding time period. Consequently, the settlement of the improved fill due to the earthquake is evaluated as approximately 8 cm at the Common factory, 14 cm at the B-packing factory and 9 cm at the C-packing factory. The settlement at the Common factory agrees well with the analytical result as shown in Figure 16. The settlement of the unimproved ground due to the earthquake is evaluated as approximately 32 cm [Hatanaka et al., 1997]. The settlement of the improved ground is reduced to almost one third of that of the unimproved ground and soil improvement by rod compaction method is activated effectively as a countermeasure during the earthquake.
The residual settlement of the unimproved ground is not consistent well with the analytical result as shown in Figure 17. The reason why the analytical result is almost one third of the actual residual settlement is that the permeability in layer B1 is relatively lower than that in layers B2 and B3. The another reason is supposed to be that the change of compressibility and permeability is occurred by means of fissure and sand boils of the fill during the earthquake.

CONCLUSIONS AND REMARKS

The liquefaction strength of the improved Masado fill by rod compaction method is one and a half time as large as that of the unimproved fill. The compression index during post-liquefaction shows almost the same value on the improved fill and the unimproved fill. The liquefaction was occurred at G.L.-7 m or deeper of the Masado fill on the improved ground, while occurred at all depth (18 m) of the Masado fill on the unimproved ground during the 1995 Hyogoken-nanbu earthquake. In both of the analytical and the actually observed results, the settlement of the improved ground is 7 through 8 cm and it is reduced against 32 cm actually observed on the unimproved ground. The soil improvement by rod compaction method resulting in higher liquefaction strength is effective to reduce damages induced by liquefaction. The residual settlement induced by liquefaction is properly predicted under the effective stress method considering the effect of soil improvement and the characteristics of compressibility of soil during post-liquefaction.

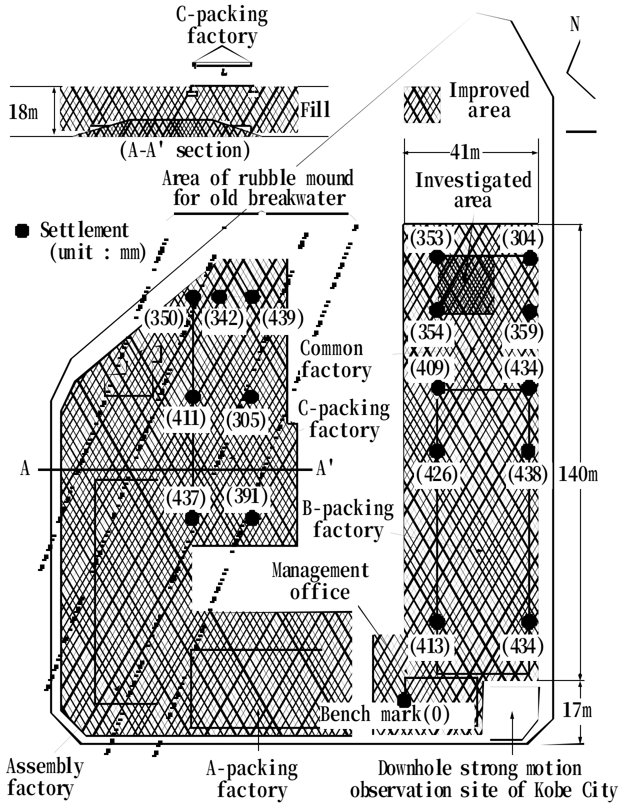

Figure 18: Residual settlement by leveling after the earthquake

ACKNOWLEDGEMENT

The authors would like to thank Messrs. organized under Geotechnical Research Collaboration Committee on the Hanshin-Awaji Earthquake.

REFERENCES

Geotechnical Research Collaboration Committee on the Hanshin-Awaji Earthquake. (1998), Annual Report of Geotechnical Research Collaboration Committee on the Hanshin-Awaji Earthquake, 1997 (in Japanese).

Hatanaka, M., Uchida, A. and Ohara, J. (1997), "Liquefaction characteristics of a gravelly fill liquefied during the 1995 Hyogo-ken nanbu earthquake", Soils and Foundations, 37 (3), pp107-115.

Ito, K. (1995), "EFECT: the code of effective stress analysis (Part I) – basic theory and constitutive model of soils –", Obayashi Corp. Technical Research Report, 51, pp7-14 (in Japanese).

Japan Road Association. (1996), Design specifications of highway bridges Part V. Seismic design.

Kobe City (1995), Report of geotechnical aspects of reclaimed fill (Port Island and Rokko Island) during the 1995 Hyogo-ken nanbu earthquake (in Japanese).

Suzuki, Y., Hatanaka, M. and Uchida, A. (1997), "Drained and undrained shear strengths of a gravelly fill of weathered granite from Kobe Port Island", Jour. of Structural and Construction Engineering, Transactions of AIJ, 498, pp67-73 (in Japanese).

Uchida, A., Hatanaka, M. and Taya, Y. (1998), "Effects of compressibility and particle crushability 0n the mechanical properties of weathered granite", IS-TOHOKU '98.

Yasuda, S., Ishihara, K., Harada, K. and Shinkawa, N. (1995), "Effect of soil improvement on ground subsidence due to liquefaction", Special Issue on geotechnical aspects of the January 17 1995 Hyogoken-Nambu earthquake, Soils and Foundations, pp99-107.